Powerful images.
Clear answers.

HOLOGIC®
The Science of Sure

Manage Patient's concerns about Atypical Femur Fracture*

Vertebral Fracture Assessment — a critical part of a complete fracture risk assessment

Advanced Body Composition® Assessment — the power to see what's inside

Visit us at ASBMR 2018 Booth #300

www.hologic.com | dxaperformance.com | 1.800.442.9892

Original Article

PiT1/Slc20a1 is required for endoplasmic reticulum homeostasis, chondrocyte survival and skeletal development[†]

Running title: PiT1 regulates ER stress in chondrocytes

Greig Couasnay, PhD[1,2,3], Nina Bon, PhD[1,2], Claire-Sophie Devignes, PhD[4,5], Sophie Sourice[1,2], Arnaud Bianchi, PhD[6,7], Joëlle Véziers, PhD[1,2,8], Pierre Weiss, PhD, DDS[1,2,8], Florent Elefteriou, PhD[3], Sylvain Provot, PhD[4,5], Jérôme Guicheux,PhD[1,2,8], Sarah Beck-Cormier, PhD[1,2, #], Laurent Beck, PhD[1,2, #]

Affiliations

[1] INSERM, UMR 1229, RMeS, Regenerative Medicine and Skeleton, Université de Nantes, ONIRIS, Nantes, F-44042 France. [2] Université de Nantes, UFR Odontologie, Nantes, F-44042 France. [3] Baylor College of Medicine, Dept. of Molecular and Human Genetics and Orthopedic Surgery, One Baylor Plaza, Houston, Texas 77030, USA. [4] INSERM UMR 1132, Centre Viggo Petersen-Hôpital Lariboisière, Paris, F-75010 France. [5] Université Paris Diderot, Sorbonne Paris-Cité, Paris, F-75010 France. [6] CNRS, UMR 7365, IMoPA, Vandœuvre-lès-Nancy, F-54505 France. [7] Université de Lorraine, Faculté de Médecine, Vandœuvre-lès-Nancy, F-54505 France. [8] CHU Nantes, PHU 4 OTONN, Nantes, F-44042 France.

[#] these authors have contributed equally to the work

Corresponding author

Laurent BECK, INSERM U1229 - RMeS, Faculté de Chirurgie Dentaire, 1 place Alexis Ricordeau, 44042 Nantes, France - email: laurent.beck@inserm.fr, Phone: +33 240 412 920

Supplementary information

Supplementary information accompanies this manuscript on the JBMR website

DOI 10.1002/jbmr.3609

Abstract

During skeletal mineralization, the sodium-phosphate co-transporter PiT1Slc20a1 is assumed to meet the phosphate requirements of bone-forming cells, although evidence is missing. Here, we used a conditional gene deletion approach to determine the role of PiT1 in growth plate chondrocytes. We show that *PiT1* ablation shortly after birth generates a rapid and massive cell death in the center of the growth plate, together with an uncompensated ER stress, characterized by morphological changes and increased *Chop*, *Atf4* and *Bip* expression. PiT1 expression in chondrocytes was not found at the cell membrane but co-localized with the ER marker ERp46, and was up-regulated by the unfolded protein response cascade. In addition, we identified the protein disulfide isomerase (Pdi) ER chaperone as a PiT1 binding partner and showed that *PiT1* ablation impaired Pdi reductase activity. The ER stress induced by *PiT1* deficiency in chondrocytes was associated with intracellular retention of aggrecan and Vegf-A, which was rescued by over-expressing a phosphate transport-deficient mutant of PiT1. Our data thus reveal a novel, Pi-transport independent function of PiT1, as a critical modulator of ER homeostasis and chondrocyte survival during endochondral ossification. This article is protected by copyright. All rights reserved

Introduction

In the skeleton, most of the bones form through endochondral ossification. During this complex and spatially regulated process, chondrocytes synthesize an abundant collagen and proteoglycan-rich extracellular matrix (ECM) template that will be ultimately calcified through the deposition of apatitic calcium-phosphate (Pi) crystals [1]. Although the precise mechanisms of crystal formation and deposition are still debated, cellular uptake of Ca and Pi by mineralizing cells is a prerequisite to the mineralization process and is tightly controlled by specialized membrane proteins [2,3].

PiT1/Slc20a1 was originally identified as a retrovirus receptor [4] and later characterized as a plasma membrane Na-dependent Pi transporter [5,6]. The skeletal expression of PiT1 and its regulation by hormonal or local chondrocytic and osteogenic differentiation factors have led to the assumption that PiT1 represents an instrumental Pi transporter during the mineralization process [7-9]. However, gathering evidence of a role of PiT1 in skeletal mineralization has been hampered by the embryonic lethality of mice lacking PiT1 [10,11]. Our initial attempt to illustrate the role of PiT1 in bone mineralization using PiT1 hypomorphic mice was also impeded by generalized anemia and incomplete *PiT1* deletion in this model [12]. Importantly, the high quantity of Pi needed for ECM mineralization is at odd with the poor transporting capacity of PiT1 [13], suggesting that the involvement of PiT1 in skeletal physiology may relate to yet unknown functions of PiT1.

The bulk of secreted or membrane-bound proteins enter the endoplasmic reticulum (ER), where they fold and assemble. When the ER protein-folding capacity is overloaded, unfolded proteins trigger the activation of intracellular signaling pathways collectively termed the unfolded protein response (UPR) [14]. The UPR up-regulates genes encoding for molecular chaperones, oxydoreductases and ER-associated degradation (ERAD) components, resulting in a reduced load of processed proteins, enhanced folding capacity and increased degradation of misfolded proteins [14]. This UPR is particularly important and robust in chondrocytes and allow them to cope with the massive load of ECM proteins synthesized in the ER. Prolonged ER-stress, however, results in an

3

UPR-dependent apoptosis, characterized by the up-regulation of CCAAT/Enhancer-Binding Protein (C/EBP) Homologous Protein (Chop) [15]. An imbalance of the folding and/or secretion of ECM proteins is involved in the pathogenesis of many connective tissue disorders such as pseudoachondroplasia (PSACH) and autosomal dominant multiple epiphyseal dysplasia (MED) [16]. XBP1 and ATF4 are two of the main transcription factors involved in mediating the UPR pathway [14]. Interestingly, the phenotype of PiT1 global knockout (KO) mice is reminiscent of *Xpb1* and *Atf4* null mice [10,17,18], which is suggestive of a yet unknown functional crosstalk between PiT1 and the UPR. This observation underscores an unidentified role of PiT1 in cartilage, which we addressed by cell-specific and temporally-controlled PiT1 ablation in the chondrocytic lineage.

Materials and Methods

Animal experimentation and ethics

Generation of $PiT1^{lox/lox}$ and $Agc1^{tm(IRES-creERT2)}$ has been described previously [10,19]. Chondrocyte-specific deletion of $PiT1$ was performed by crossing $PiT1^{lox/lox}$ to $Agc1^{CreERT2/+}$; $PiT1^{lox/+}$ mice to generate littermate control ($Agc1^{+/+};PiT1^{lox/lox}$) and mutant ($Agc1^{CreERT2/+}$; $PiT1^{lox/lox}$) mice that were injected intra-peritoneally with 300µg of tamoxifen (Sigma-Aldrich) at 3-days of age (P3). Thereafter in the manuscript, $Agc1^{+/+};PiT1^{lox/lox}$ mice are denoted «Ctrl», whereas $Agc1^{CreERT2/+}$; $PiT1^{lox/lox}$ mice are denoted «$PiT1^{cKO}$». To ensure that the observed phenotype did not originate from an artifactual Cre and/or tamoxifen effect, additional control mice were obtained from $Agc1^{CreERT2/+};PiT1^{lox/+}$ x $PiT1^{lox/+}$ crossings to generate Cre-positive $PiT1^{+/+}$ mice ($Agc1^{CreERT2/+}$; $PiT1^{+/+}$) that were injected with tamoxifen. No difference could be seen between these additional control mice and the Cre-negative ($Agc1^{+/+}$; $PiT1^{lox/lox}$) control mice used in this study. In addition, no difference could be seen between tamoxifen-injected control animals (both Cre-negative and Cre-positive control mice) and mice that were not injected with tamoxifen. Genomic DNA from tail was used for PCR genotyping. Primers used to assess allelic recombination by PCR are reported in Table S1. Animal care and maintenance were provided through the University of Nantes accredited animal facility at the "Unité de Thérapeutique Expérimentale" (Nantes). Mice were viable, fertile and bred normally and were housed under pathogen-free conditions. All procedures were approved by the Animal Care and Use Committee of the Région Pays de la Loire and conducted according to the French and European regulations on care and protection of laboratory animals (EC Directive 86/609, French Law 2001-486 issued on 6 June 2001) and to the National Institutes of Health Animal Welfare (project #02286.02).

Tissue sample processing and histological staining

Humerus were fixed in 4% paraformaldehyde in phosphate buffer saline (PBS, Thermo Fisher Scientific) during 24h to 48h and decalcified in 0.5M EDTA pH 8.0 before being embedded in

paraffin (Leica TP1020 automated tissue processor). Serial 4 μm-thick sections histological staining or immunohistochemistry were obtained using a microtome (Microtome 2050® - Reichert Jung). Staining of sections with Alcian blue, Harris' hematoxylin and Safranin-O were carried out using standard histological procedures, as described earlier [12].

Immunohistochemistry (IHC) and TUNEL assay

Paraffin embedded sections were processed for IHC as previously described [10]. Specific antigen retrieval conditions and list of antibodies used are reported in Table S2. Stained sections were then mounted with Eukitt® and scanned using a Hamamatsu NanoZoomer HT (Hamamatsu Photonics KK) digital scanner at a 40x magnification.To reveal apoptotic cells, the DeadEndTM fluorometric TUNEL system (Promega) was used according to the manufacter's instructions.

Cell culture and immunofluorescence studies

Primary chondrocytes were isolated from *PiT1*[cKO] mice as described previously [20] and cultured in Dulbecco's modified Eagle's medium (DMEM) supplemented with 10% FBS. Undifferentiated ATDC5 cells were maintained in DMEM:F12 medium supplemented with 5% FBS. For differentiation experiments, ATDC5 were cultured in cell monolayer during 28 days in DMEM:F12 medium supplemented with 5% FBS in presence of 10 μg/mL bovine insulin, 10 μg/mL human transferrin, and 3x10-8 M sodium selenite, as previously described [21]. HEK293T cells were maintained in DMEM supplemented with 10% FBS. For immunofluorescence studies, cells were fixed in cold methanol and blocked in 1% bovine serum albumin in PBS during 1h at room temperature (RT). Incubations with specific antibodies were performed overnight at 4°C. The list of antibodies used is reported in Table S2. Images were acquired with a confocal microscope (Nikon Eclipse C1).

Transfections and transductions

For lentiviral-based deletion of *PiT1*, shRNA targeting *PiT1* and shScramble sequences [22] were introduced in the pSicoR backbone (Addgene). ATDC5 were infected with lentiviruses

overnight and the media were refreshed on the next morning. To over-express the transport-deficient mutant of PiT1, the S621A mutation was introduced into the *PiT1* sequence [22] and the DNA constructs containing either wild-type (WT) PiT1 or PiT1 S621A were inserted in the lentiviral vector pHAGE-CMV-MCS-IRES-ZsGreen (PlasmID Repository, Harvard Medical School). Viral infection was conducted as described above. To transiently inactivate UPR transcription factors, ATDC5 cells were transfected with sequence specific siRNAs (100nM) from Dharmacon (Chicago, IL) using oligofectamine (Thermo Fisher Scientific). Transductions and transfections were also conducted in primary chondrocytes. To rescue the Vegf-A cellular retention, primary chondrocytes were transfected with the transport-deficient mutant plasmid PiT1 S621A using JetPrime (PolyPlus transfection, Illkirch, France), as per manufacturer's instructions.

Gene Expression Analysis

Total RNA was isolated from cells or tissues using the Nucleospin® RNA II kit (Macherey-Nagel, Germany) according to the manufacturer's instructions. RNA was reverse transcribed using SuperScript®III (Thermo Fisher Scientific) as per manufacturer's instructions. Real-time PCR (qPCR) was performed on a Bio-Rad CFX96 using SYBR®Select Master Mix (Thermo Fisher Scientific). Primer efficiency was determined using a standard curve with a 1:4 dilution and specificity of amplification was verified from the melting curve analysis. Expression of target genes were normalized to pinin (*Pnn*) or glucuronidase B (*GusB*) expression levels and the relative gene expression levels were calculated as previously described [23]. The sequences of primers used in this study are listed in Table S3. Analysis of *Xbp1* splicing was performed by RT-PCR using the following primers: 5'-GAACCAGGAGTTAAGAACACG-3' and 5'-AGGCAACAGTGTCAGAGTCC-3'.

Immunoblot analysis

Cells were lysed for 30 min in ice-cold lysis buffer (150 mM NaCl, 10 mM Tris HCl pH 8, 5 mM EDTA, 1% NP40, 0.1% SDS, 0.5% Na-deoxycholate and a protease inhibitor cocktail from

7

Roche), the protein extract was resolved by NuPAGE© Novex 4-12% SDS-PAGE (Thermo Fisher Scientific) and electro-blotted onto PVDF membranes. After blocking with non-fat dry milk/TBST, blots were probed with primary and secondary HRP antibodies and revealed with ChemiDoc Imaging SystemTM (Bio-Rad). The list of antibodies and the specific experimental conditions used in this study are reported in Table S2.

Co-immunoprecipitation

Transfected ATDC5 cells were washed with ice-cold PBS, and lysed with lysis buffer (50 mM NaCl, 1% Nonidet P-40, 20 mM EDTA, 0.5% sodium deoxycholate, 50 mM Tris HCl, pH8, and proteasephosphatase inhibitor cocktail). Cell debris were removed by centrifugation at 14,000g for 10 min.Equal amounts of cell lysates were used for immunoprecipitation with anti-PiT1 or anti-Pdi using protein A/G ultralink resin (Thermo Fisher Scientific). Immunoprecipitates were washed four times with lysis buffer, boiled in Laemmli buffer, and immunoblotting was performed as described above.

ELISA

Determination of Vegf-A in supernatant of primary chondrocytes was performed with the Murine Vegf Mini ABTS ELISA Development Kit (Peprotech). The Vegf-A levels were normalized with total protein content in each sample.

Transmission electron microscopy (T.E.M.)

Samples were harvested and fixed (2% glutaraldehyde, 0.2 M sodium cacodylate buffer pH 7.2) for 1h30 at 4°C, then washed overnight at 4°C in 0.2 M sodium cacodylate buffer pH 7.2. Post fixation was carried out with 2% osmium for 1h, and samples were washed three times in distilled water. Samples were dehydrated in ethanol, washed with propylene oxide twice for 15 min and impregnated with a 1:1 ratio of propylene oxide:epon overnight. This was then replaced with 100% of epon during 5h before polymerization performed during 24h at 37°C and 48h at 60°C. Ultra-thin

8

sections (70-80 nm) were examined with a JEM-1010 microscope (JEOL), operating at an accelerated voltage of 80 kV.

Yeast two-hybrid screen

Yeast experiments were performed by Hybrigenics (Paris, France). The library used for the screen was isolated from human placenta. The large intracellular loop (denominated iLoop1 thereafter) of human PiT1 (from amino acid 250 to 510) was used as a bait for the screen since the largest sequence differences between PiT1 and PiT2 were found in this region of the protein.

Expression and purification of murine iLoop1

The sequence corresponding to amino-acids 250-510 of murine PiT1 (iLoop1) was cloned into the expression vector pcDNA6 V5-6His using Fastcloning [24]. HEK293T cells were transfected with 1µg pcDNA6-iLoop1 plasmid and iLoop1 was purified using a EN-NTA spin columns kit (Qiagen), following manufacturer's instructions. Briefly, cells were lysed 48h after transfection in 50 mM NaH2PO4, 300 mM NaCl, 10 mM imidazole pH 8.0. After lysate clearing by centrifugation, the supernatant was loaded on nickel-chelating resin NTA and iLoop1 was eluted in a 500 mM imidazole. Dialysis of purified protein was performed overnight at 4°C in a saline buffer (150 mM NaCl and 20 mM Tris-HCl pH 7.5) to remove imidazole.

Pdi activity assay

Pdi activity was monitored as described [25]. ATDC5 cells were harvested, resuspended in a suspension buffer (50 mM Tris-HCl pH 7.5, 25 mM KCl and 5 mM MgCl2) sonicated and centrifuged at 11,000 g for 10 min. Proteins were added in 200 µL of reaction mix (100 mM potassium phosphate pH 7.0, 2 mM EDTA pH 7.5, 100 µM bovine insulin and 2 mM DTT) and Pdi activity was monitored as measured by increased turbidity at O.D. 660 nm during 30 min. Controls containing recombinant PDI, reaction buffer and insulin substrate, but no ATDC5 cells lysate were used as a blank. The OD660 value of this blank was subtracted to experimental values obtained with ATDC5 cells lysates.

Bioinformatics analysis

Transcription factor binding site prediction was performed on the proximal 5-kb region of the murine *PiT1* promoter using MatInspector software suite (Genomatix). Conservation of ER stress putative binding sites was analyzed using the UCSC genome browser (genome version mm9) 60-way Conservation track [26].

Statistics

Data are expressed as mean ± S.E.M. Unless otherwise stated, experiments were repeated at least three times. Depending on the number of samples and their distribution, results were analyzed using a one-way ANOVA, unpaired Student's t test or a non-parametric Mann and Whitney test. A *p* value of less than 0.05 was considered significant (* *p*<0.05; ** *p*<0.01). Statistical analysis was performed with the GraphPad Prism 5.0 software.

Results

Targeted disruption of PiT1 in chondrocytes impairs endochondral ossification

To investigate the role of PiT1 in endochondral ossification, we crossed conditional *PiT1^{lox/lox}* mice [10] with *Agc1^{tm(IRES-creERT2)}* transgenic mice [19] to generate *PiT1^{lox/lox};Agc1^{tm(IRES-creERT2)}* mutant mice (denominated *PiT1^{cKO}* thereafter) (Supplemental Fig. 1*A*). We injected pups with tamoxifen at postnatal day 3 (P3) to induce the Cre-mediated deletion of *PiT1* exon 5, leading to PiT1 functional invalidation in femoral epiphyses as soon as 8 hours post-tamoxifen injection (p.i.) (Supplemental Fig. 1*B*) [10]. Cre induction was associated with a stable decrease in mRNA expression encoding the wild-type PiT1 in epiphysis chondrocytes over-time (Supplemental Fig. 1*C*), and with a rapid decrease in PiT1 protein abundance in *PiT1^{cKO}* chondrocytes (Fig. 1*A*). PiT1 ablation did not lead to over-expression of the PiT1 paralog PiT2 (Fig. 1*A* and Supplemental Fig. 1*D*), thus excluding a possible PiT2-driven compensatory mechanism. Histological analyses of proximal humerus epiphyses 7 days p.i. revealed the presence of an inverted drop-like shaped hypocellular zone in the center of the growth plate of *PiT1^{cKO}* mice (Fig. 1*B*), which was visible as soon as 24h p.i. (Supplemental Fig. 1*E*). Twelve days later, this hypocellular zone had disappeared and a reduction in the area of the type X collagen positive hypertrophic layer could be observed (the percentage of hypertrophic area *vs* total growth plate area was 18.9±0.6% in WT and 14.6±3% in cKO) (Fig. 1*B*). Consistent with these growth plate abnormalities, the expression of chondrocytic markers in primary cultures of *PiT1*-depleted chondrocytes and in *PiT1*-depleted ATDC5 chondrogenic cell line decreased significantly, as did the synthesis of glycosaminoglycan synthesis (Fig. 1*C-E*).

The cellular growth plate abnormalities caused by post-natal deletion of *PiT1* in cartilage resulted in reduced body size and weight (Fig. 1*F*). Since PiT1 has been characterized as a phosphate transporter [5] and phosphate is an essential component of hydroxyapatite crystals, we investigated the mineralization of the mutant growth plate and bones of control and mutant P22 mice by Von Kossa and Trichrome-Masson staining. Quantification of the cortical and trabecular

mineralized area showed no difference between genotypes, and no overt osteoidosis was observed in mutant bones (Supplemental Fig. 1*F* and data not shown). When chondrocytes isolated from control and mutant mice were cultured using 3D high-density micromasses, no difference in mineralization and expression of genes involved in mineralization pathways, such as *Alpl* and *Phospho1*, was detected (Supplemental Fig. 1*G-H*), suggesting the absence of chondrocyte-autonomous defect in mineralization mechanisms. Overall, these data support the idea that PiT1 is required for the growth plate maturation process, but not for the mineralization potential of growth plate chondrocytes.

PiT1 depletion in cartilage induces ER-stress and chondrocyte death

To understand the growth plate defect observed in PiT1 mutant mice, we analyzed mutant growth plates early after tamoxifen injection. Eight hours following PiT1 ablation, alcian blue staining of proximal humeri revealed intracellular glycosaminoglycan retention in P3 *PiT1*^{cKO} chondrocytes, specifically in the center of the growth plate (Fig. 2*A*). This was associated with a swelling of cells, with no change in type II and X collagen immunostaining (Supplemental Fig. 2*A-B*). In central growth plate chondrocytes, aggrecan was retained within the cells and co-localized with the ER marker ERp46 (as shown by confocal microscopy and the white arrows in Fig. 2*B*), whereas other matrix proteins such as Cartilage oligomeric protein (COMP) were not retained (Supplemental Fig. 2*C*). Consistent with the retention of aggrecan, a low content of alcian blue-stained extracellular mature glycosaminoglycans was observed 48 hours post-ablation in the center of *PiT1*^{cKO} growth plate (Fig. 2*C*). No significant difference in the proportion of BrdU-positive chondrocytes was detected between control and *PiT1*^{cKO} growth plates 48 hours or 7 days post PiT1 ablation (Supplemental Fig. 2*D*). In contrast, TUNEL analyses showed a massive cell death specifically in the center of mutant growth plates 3 days post *PiT1* ablation (Fig. 2*D*), underscoring the role of PiT1 in chondrocyte survival. The effect of *PiT1* deletion on chondrocyte survival was visible as early as 8h p.i. and was not observed in the hypertrophic layer (Supplemental Fig. 2*E*),

nor in absence of terminal deoxytransferase (negative control, Supplemental Fig 2*F*). In addition, when examining the spatial expression of *Sox9* and *Pth1r*, which are well known to control the synchronization of chondrocyte differentiation with other critical processes of endochondral bone development, such as cartilage matrix mineralization, we did not observe major differences between genotypes (Supplemental Fig. 3). These data indicate that deletion of *PiT1* post-natally, although not overtly altering bone growth and mineralization, induces a transient and localized phenotype in the hypoxic region of the growth plate, at a stage characterized by sustained ECM synthesis and bone growth.

The accumulation of aggrecan in the ER of mutant cells and the cell death associated with PiT1 loss-of-function suggested that *PiT1^cKO^* growth plate chondrocytes may experience an uncompensated ER stress. To address this possibility, we performed ultrastructural analyses by transmission electron microscopy (T.E.M.) 8h post-tamoxifen injection. Transverse semi-thin sections of humerus epiphyses showed a well-developed and organized rough ER in both the peripheral and central zones of the WT growth plate (Fig. 2*E-F*, upper panels), whereas *PiT1^cKO^* growth plates presented with a mild distended ER in the peripheral zone but a more distended and fragmented ER in central zone mutant chondrocytes (Fig. 2*E-F*, lower panels), which are both a hallmark of ER-stressed cells. The ER stress experienced by PiT1-depleted growth plate chondrocytes *in vivo* was also revealed by the strong central expression of Chop, one of the main target of the UPR pathway activated during ER stress [27] (Fig. 2*G* and Supplemental Fig. 4*A*), and the increase of the UPR-activated protein caspase-12 staining throughout the growth plate [28] (Fig. 2*G* and Supplemental Fig. 4*B*). In cultured ATDC5 cells, shRNA-mediated *PiT1* depletion further supported these results by showing a distended ER network (Supplemental Fig. 4*C*) and increased Chop and Casp12 protein expression (Supplemental Fig. 4*D*). In addition, *Chop, Atf4* and *Bip* expression was increased in PiT1^cKO^ chondrocytes compared to controls (Fig. 2*H*). The splicing of the ER stress marker *Xbp1* was also increased in *shPiT1*-transduced chondrocytes, thus confirming that depletion of PiT1 triggered ER stress (Fig. 2*I*). ShRNA-mediated PiT1 depletion increased

13

Chop mRNA while over-expression of a Pi transport-deficient mutant of PiT1 [22,29] led to the opposite effect (Fig. 2*J*), suggesting that ER homeostasis is modulated by PiT1 independently from its Pi transport function.

PiT1 is an ER-stress regulated gene modulating Pdi activity

To further determine the role of PiT1 in ER homeostasis, we investigated its expression in the ER and its regulation by the UPR pathway. Immunofluorescence analyses performed in ATDC5 cells revealed that PiT1 mainly co-localized with the ER marker ERp46, suggesting that it was mainly expressed in the ER compartment (Fig. 3*A*). When ATDC5 cells were stimulated with the ER stress inducer tunicamycin during 8h or 24h, *Chop* mRNA and protein levels were significantly increased, as expected, but PiT1 expression was found up-regulated as well (Fig. 3*B* and Supplemental Fig. 5*A*). In line with this result, blocking the expression of the main UPR transcription factors XBP1s, ATF6N and ATF4 repressed the expression of *PiT1* in tunicamycin-treated cells (Fig. 3*C*). Furthermore, we identified evolutionary conserved putative binding sites for XBP1s, ATF6N and ATF4 in the proximal 1-kb region of the mouse *PiT1* promoter (Supplemental Fig. 5*B*). Lastly, when the 5'-flanking region of the *PiT1* gene was inserted upstream of a luciferase reporter gene sequence, it was able to be transactivated by UPR mediators: although XBP1s alone was not able to transactivate the *PiT1* promoter, ATF4 and ATF6N increased the basal activity of the *PiT1* promoter 4- and 2.5-fold over controls, respectively (Supplemental Fig. 5*C*). Collectively, these data identify PiT1 is an ER stress-regulated gene.

To get a better insight into the role of PiT1 during ER homeostasis, we searched for potential PiT1 protein partners using a yeast two-hybrid screen method. Using this approach, we identified 20 potential PiT1 partners, among which the Protein Disulfide Isomerase family A member 1 (Pdi), stood out, as a high confidence prey (Supplemental Fig. 5*D*). Since Pdi was described as a major ER chaperone involved in the folding of nascent peptides [30], we investigated further the functional link between PiT1 and Pdi. We first confirmed the physical interaction between PiT1 and Pdi under

14

basal conditions by co-immunoprecipitation in ATDC5 chondrocytes (Fig. 3*D* and Supplemental Fig. 6). Interestingly, the immunoprecipitation results supported an increase in PiT1-Pdi interaction under ER stress conditions. In PiT1-depleted cells, ER-stress did not impact the mRNA and protein expression, and cellular localization of Pdi (Supplemental Fig. 5*E-G*), but did reduce Pdi activity compared to control cells (Fig. 3*E*), as measured by a Pdi activity assay based on the aggregation of the insulin B chain following its reduction by Pdi [25]. To confirm that PiT1 modulates Pdi activity, we performed a dose response experiment in a cell-free system containing purified Pdi and various quantities of purified iLoop1, the large intracellular loop of PiT1 that was used as a bait in the yeast two-hybrid screen. Measuring solution turbidity as an indication of the insulin B chain aggregation induced by Pdi activity, we observed a dose-dependent increase in Pdi activity (Fig. 3*F*). Altogether, these results strongly suggest that PiT1 is an ER stress regulated gene that stimulates the activity of the ER chaperone Pdi. Therefore it is expected that in case of PiT1 depletion, the resulting decrease in Pdi activity would cause an ER stress, triggering the UPR.

The ER-stress caused by PiT1 deficiency is associated with decreased Vegf-A secretion in the central hypoxic region of the growth plate

The uncompensated ER-stress triggered by PiT1 deletion occurred mainly in the central region of the epiphysis, which is known to be hypoxic [31], thus suggesting a possible functional interaction between PiT1, the hypoxia pathway and its main target vascular endothelial growth factor A (Vegf-A). Immunofluorescence analysis of *PiT1cKO* growth plates 8h post PiT1 ablation showed intense Vegf-A staining in chondrocytes from the central epiphysis region compared to controls and to the non-hypoxic region of the same growth plate (Fig. 4*A*), which arose in absence of induction of epiphyseal *Vegf-A* mRNA expression (Fig. 4*B*). The latter may be due to the relative small size of the central hypoxic zone compared to the rest of the epiphysis. However, when primary chondrocytes from both control and *PiT1cKO* mice were cultured in low oxygen tension (1%), *Vegf-A* and *Pgk1* mRNA expression was up-regulated in control and *PiT1cKO* cells (Fig. 4*C*),

suggesting that *PiT1* deletion in growth plate chondrocytes does not impair cell response to hypoxia. However, hypoxia reduced the expression of *PiT1* in WT chondrocytes (Fig. 4*C*) and increased the expression of UPR markers both in Control or PiT1-depleted cells (Supplemental Figure 7*A*). Together, these data suggest that both the deletion of *PiT1* (induced genetically in *PiT1^cKO* mice) and the hypoxic condition of the central growth plate area (leading to further reduced *PiT1* expression) contribute to the uncompensated ER-stress leading to impaired Vegf-A secretion. Further supporting the idea that PiT1 depletion impairs Vegf-A secretion, we detected a decrease in Vegf-A secretion in the supernatant of PiT1-depleted primary hypoxic chondrocytes by ELISA (Fig. 4*D*), associated with an increase in cellular Vegf-A protein content (Supplemental Fig. 7*B*, comparing lane 5 to lane 12). Importantly, we could rescue the high Vegf-A cellular content of PiT1-depleted chondrocytes by re-expressing a phosphate transporter-deficient form of PiT1 (Fig. 4*E*, and Supplemental Fig. 7*B* comparing lane 12 to lanes 13 and 14). Collectively, these data support a model whereby in the hypoxic environment typical of the central growth plate, PiT1 is required for normal ER homeostasis and secretion of factors crucial for growth plate homeostasis, independently of its Pi transport function.

Discussion

In the present study, we identified a role of PiT1 in ER homeostasis maintenance during endochondral ossification via detailed analysis of a chondrocyte-specific and temporally-controlled PiT1 deficient mouse model. We show that PiT1 in chondrocytes is mainly expressed in the ER, and not at the cell surface, thus challenging its role as the main phosphate transporter in this cell lineage, and strengthening its role in ER homeostasis. Accordingly, we show that PiT1 expression is up-regulated under ER stress conditions, a feature shared by genes involved in UPR-related events. In addition, we show that PiT1 expression is regulated by the three main UPR transcription factors and mainly by ATF4, a finding consistent with a recent study conducted in vascular smooth muscle cells [32]. The importance of PiT1 in ER homeostasis is further documented by i) its interaction with Pdi, an ER chaperone strongly induced in ER-stress conditions and involved in the formation of disulfide bonds in newly synthesized proteins [30,33,34], ii) the dose-dependent modulation of Pdi reductase activity by PiT1, and iii) the impaired secretion of proteoglycans and Vegf-a in PiT1-deficient chondrocytes in the hypoxic center of the growth plate.

Interplay between PiT1, ER homeostasis and hypoxia

While genes involved in UPR are known to mediate the response to unfolded or misfolded proteins in the ER, they have also been described to be required for the maturation of chondrocytes during endochondral ossification [35]. For instance, *Atf4* deficiency in chondrocytes leads to delayed endochondral ossification, short stature and disorganization of the growth plate [36]. Similarly, disruption of *Xbp1* leads to delayed ossification [37], whereas overexpression of *Xbp1* in ATDC5 chondrocytes increases the expression of the hypertrophic markers ColX and *Runx2* [38]. Moreover, since Atf4 has been shown to be involved in other integrated stress responses, the regulation of PiT1 by this transcription factor may reveal roles in other physiological mechanisms [32,39].

Interestingly, the decrease in Pdi activity and increase in ER-stress detected in *PiT1^{cKO}* chondrocytes are associated with reduced expression of chondrocyte differentiation markers, in line

17

with the notion that ER stress and the UPR pathway are critical for adequate growth plate maturation during endochondral bone formation. Although more work is needed to understand the mechanistic link between PiT1, Pdi, endochondral bone formation and ER stress, our experiments (Figure 3*D* and Supplemental Figure 5*D*) suggested that the Pdi chaperone may interact with the fourth intracellular loop of PiT1 (iLoop1) through its b'-x-linker-a' hinged motif [40,41]. This specific region of Pdi is involved in a pH-dependent conformational change during ER stress allowing its preferential interaction with reduced/unfolded or mis-oxidized proteins [34]. Hence, an interaction of PiT1 with the b'-x-linker-a' region would interfere with Pdi activity and explain the dose-dependent PiT1 modulation of Pdi reductase activity reported herein. Although the lack of reliable PiT1 antibody for IHC prevents the possibility to study PiT1-Pdi co-localization in different physiological conditions, one can imagine that if PiT1 depletion leads to a decrease in Pdi activity, it is expected that this deletion results in a global unbalance of ER folding capacity of chondrocytes, leading to a global defect in protein secretion. However, our data showed that PiT1 depletion in chondrocytes led to an intracellular accumulation of aggrecan but not collagen or COMP, arguing against this idea. Similarly, defects in the secretion of Vegf-A, but not transforming growth factor-ß (Tgf-ß) or growth/differentiation factor 5 (Gdf5) were observed (Supplemental Fig. 7*C-D*), indicating that chondrocytic secretion is not globally affected in absence of PiT1. Although more investigation are needed to decipher the underlying mechanisms, this observation may be consistent with the existence of distinct ER sorting mechanisms for different matrix molecules, as shown in chondrocytes of pseudoachondroplasia patients (PSACH) and in other studies [42-44].

The defect in chondrocyte differentiation observed in cKO mice may also result in part from indirect consequences of PiT1 deletion, such as cell death in the hypoxic central zone. Indeed, phenotypic analysis of *PiT1^cKO* growth plates showed that uncompensated ER-stress was visible throughout the entire epiphysis of mutant mice, with no loss of cell viability under normal oxygen tension conditions. This indicated that the uncompensated ER-stress phenotype alone was not sufficient to affect the survival of mutant chondrocytes. Therefore, it is likely that the absence of

18

PiT1 in growth plate chondrocytes, associated with the low oxygen tension present in the central area of the mutant growth plates result in a loss of cell survival. This observation is reminiscent of the ER-stress induced upon deletion of *Hif1α* that caused cell death in the hypoxic cartilage [45]. It is therefore possible that instead of a global uncompensated ER stress known to trigger cell death [46], a specific change in the quality of ECM proteins synthesized by chondrocytes and a defect in Vegf-A secretion may be involved, since these factors are crucial for chondrocyte survival [45,47,48].

PiT1 mechanism of action

Although more work remains to be done to discriminate between the specific roles of each player, it is noteworthy that we were able to reduce the defect in UPR and rescue the Vegf-A secretion defect by over-expressing a transport-deficient PiT1 mutant in PiT1-depleted chondrocytes. This argues against a major role of PiT1-driven Pi transport in the observed ER phenotype, and is consistent with 1) the weak expression of this transporter at the extracellular plasma membrane and 2) the absence of abnormal mineralization in the bone of cKO mice. This also complements the growing evidence that PiT1 is a membrane-associated protein whose functions go beyond its previously established role of Na-Pi co-transporter [5,6]. Indeed, this historical function led the scientific community to hypothesize that PiT1 could mediate the transport of Pi necessary for the mineralization of the skeleton. However, *in vivo* experiments using transgenic mice over-expressing PiT1 [49] or genetically modified mouse models under-expressing PiT1 [12] have failed to demonstrate a major contribution of this transporter to mineralization processes. This data are in line with our current observation that deleting PiT1 in cartilage does not impact mineralization *per se*.

Pi-transport dependent and independent actions of PiT1 have already been described, and are not shared by its paralog PiT2. PiT1 is involved in very diverse cellular processes, such as cell proliferation and adhesion [22,50,51], tumor necrosis factor (TNF)-induced apoptosis [29], or Pi-dependent activation of the ERK1/2 MAPK pathway [52-54]. PiT1 is also involved in pathological vascular calcifications [55], liver development [10], erythroid and B cell differentiation [10,56,57], and

19

enhanced insulin signaling and decreased hepatic lipogenesis [58]. Based on these observations, we hypothesized that the multi-functional nature of PiT1 comes from the recruitment or sequestration of specific cellular proteins, which can modulate their activities. Since the largest protein sequence differences between PiT1 and PiT2 are found in their large cytoplasmic iLoops [22], which is not involved in Pi-transport function [59-62], we conducted a two-hybrid screen leading to the identification of Pdi as a PiT1 protein partner. Our results are consistent with the possibility that the Pi-transport function of PiT1 does not contribute to the observed phenotype, but rather that PiT1 helps maintaining ER homeostasis through its binding to Pdi. A defect in PiT1-Pdi interaction would decrease Pdi activity, leading to an uncompensated ER stress, which, in the central hypoxic region of the growth plate, would lead to secretion defects of Vegf-A and aggrecan, and subsequent cell death. As discussed above, more investigations are required to determine the impact of PiT1 deletion on distinct secretory pathways or ER-sorting mechanisms, and to identify what other secreted molecules might be affected. Another aspect to take into consideration when trying to define the role and mode of action of PiT1 in chondrocytes, is the fact that our data were obtained using an inducible Cre mouse model. It is possible that the phenotypical consequences of PiT1 deletion earlier in development would diverge from our observations leading to abnormal skeletal development.

In summary, our work reveals a novel Pi-independent function of PiT1 in the regulation of ER homeostasis in chondrocytes, necessary for the maintenance of growth plate chondrocyte differentiation and survival during endochondral ossification.

Acknowledgements

Authors' roles

Study design: GC, NB, AB, SP, SB-C, and LB

Study conduct: BJK, YM, NAS, and CSK

Data collection: GC, NB, C-SD, SS, AB, JV, and SB-C

Data analysis: GC, NB, C-SD, AB, JV, FE, SP, SB-C, and LB.

Data interpretation: GC, NB, FE, SP, JG, SB-C, and LB.

Drafting manuscript: GC, FE and LB

Revising manuscript content: GC, NB, C-SD, FE, SP, SB-C and LB

Approving final version of manuscript: all authors.

LB takes responsibility for the integrity of the data analysis.

Conflict of interest

All authors state that they have no conflicts of interest

References

1.   Wuthier RE. Involvement of cellular metabolism of calcium and phosphate in calcification of avian growth plate cartilage. J Nutr. 1993 Feb;123(2 Suppl):301–9.

2.   Suzuki A, Ghayor C, Guicheux J, Magne D, Quillard S, Kakita A, Ono Y, Miura Y, Oiso Y, Itoh M, Caverzasio J. Enhanced expression of the inorganic phosphate transporter Pit-1 is involved in BMP-2-induced matrix mineralization in osteoblast-like cells. J Bone Miner Res. 2006 May 1;21(5):674–83.

3.   Mahamid J, Addadi L, Weiner S. Crystallization Pathways in Bone. Cells Tissues Organs. 2011 ed. 2011;194(2-4):92–7.

4.   O'Hara B, Johann SV, Klinger HP, Blair DG, Rubinson H, Dunn KJ, Sass P, Vitek SM, Robins T. Characterization of a human gene conferring sensitivity to infection by gibbon ape leukemia virus. Cell Growth Differ. 1990 Mar;1(3):119–27.

5.   Kavanaugh MP, Miller DG, Zhang W, Law W, Kozak SL, Kabat D, Miller AD. Cell-surface receptors for gibbon ape leukemia virus and amphotropic murine retrovirus are inducible sodium-dependent phosphate symporters. Proc. Natl. Acad. Sci. U.S.A. 1994 Jul 19;91(15):7071–5.

6.   Miller DG, Miller AD. A family of retroviruses that utilize related phosphate transporters for cell entry. J Virol. 1994 Dec;68(12):8270–6.

7.   Nielsen LB, Pedersen FS, Pedersen L. Expression of type III sodium-dependent phosphate transporters/retroviral receptors mRNAs during osteoblast differentiation. Bone. 2001 Jan 24;28(2):160–6.

8. Palmer G, Zhao J, Bonjour J, Hofstetter W, Caverzasio J. In vivo expression of transcripts encoding the Glvr-1 phosphate transporter/retrovirus receptor during bone development. Bone. 1999 Jan;24(1):1–7.

9. Yoshiko Y, Candeliere GA, Maeda N, Aubin JE. Osteoblast autonomous Pi regulation via Pit1 plays a role in bone mineralization. Mol Cell Biol. 2007 Jun 1;27(12):4465–74.

10. Beck L, Leroy C, Beck-Cormier S, Forand A, Salaün C, Paris N, Bernier A, Urena-Torres P, Prié D, Ollero M, Coulombel L, Friedlander G. The phosphate transporter PiT1 (Slc20a1) revealed as a new essential gene for mouse liver development. PLoS ONE. 2010;5(2):e9148.

11. Festing MH, Speer MY, Yang H-Y, Giachelli CM. Generation of mouse conditional and null alleles of the type III sodium-dependent phosphate cotransporter PiT-1. Genesis. 2009;47(12):858–63.

12. Bourgine A, Pilet P, Diouani S, Sourice S, Lesoeur J, Beck-Cormier S, Khoshniat S, Weiss P, Friedlander G, Guicheux J, Beck L. Mice with hypomorphic expression of the sodium-phosphate cotransporter PiT1/Slc20a1 have an unexpected normal bone mineralization. PLoS ONE. 2013;8(6):e65979.

13. Virkki LV, Biber J, Murer H, Forster IC. Phosphate transporters: a tale of two solute carrier families. Am J Physiol Renal Physiol. 2007 Jul 18;293(3):F643–54.

14. Walter P, Ron D. The Unfolded Protein Response: From Stress Pathway to Homeostatic Regulation. Science. 2011 Nov 24;334(6059):1081–6.

15. Tsang KY, Chan D, Cheslett D, Chan WCW, So CL, Melhado IG, Chan TWY, Kwan KM, Hunziker EB, Yamada Y, Bateman JF, Cheung KMC, Cheah KSE. Surviving endoplasmic reticulum stress is coupled to altered chondrocyte differentiation and function. PLoS Biol. 2007 Mar;5(3):e44.

16. Boot-Handford RP, Briggs MD. The unfolded protein response and its relevance to connective tissue diseases. Cell Tissue Res. 2009 Oct 23;339(1):197–211.

17. Reimold AM, Etkin A, Clauss I, Perkins A, Friend DS, Zhang J, Horton HF, Scott A, Orkin SH, Byrne MC, Grusby MJ, Glimcher LH. An essential role in liver development for transcription factor XBP-1. Genes Dev. 2000 Jan 15;14(2):152–7.

18. Masuoka HC, Townes TM. Targeted disruption of the activating transcription factor 4 gene results in severe fetal anemia in mice. Blood. 2002 Feb 1;99(3):736–45.

19. Henry SP, Jang CW, Deng JM, Zhang Z, Behringer RR, de Crombrugghe B. Generation of aggrecan-CreERT2 knockin mice for inducible Cre activity in adult cartilage. Genesis. 2009 ed. 2009 Dec;47(12):805–14.

20. Gosset M, Berenbaum F, Thirion S, Jacques C. Primary culture and phenotyping of murine chondrocytes. Nat Protoc. 2008;3(8):1253–60.

21. Julien M, Magne D, Masson M, Rolli-Derkinderen M, Chassande O, Cario-Toumaniantz C, Cherel Y, Weiss P, Guicheux J. Phosphate stimulates matrix Gla protein expression in chondrocytes through the extracellular signal regulated kinase signaling pathway. Endocrinology. 2007 Feb 1;148(2):530–7

22. Beck L, Leroy C, Salaün C, Margall-Ducos G, Desdouets C, Friedlander G. Identification of a novel function of PiT1 critical for cell proliferation and independent of its phosphate transport activity. J Biol Chem. 2009 Nov 6;284(45):31363–74.

23. Schmittgen TD, Livak KJ. Analyzing real-time PCR data by the comparative C(T) method. Nat Protoc. 2008;3(6):1101–8.

24. Li C, Wen A, Shen B, Lu J, Huang Y, Chang Y. 1472-6750-11-92. BMC Biotechnol. BioMed Central Ltd; 2011 Oct 12;11(1):92.

25. Lovat PE, Corazzari M, Armstrong JL, Martin S, Pagliarini V, Hill D, Brown AM, Piacentini M, Birch-Machin MA, Redfern CPF. Increasing melanoma cell death using inhibitors of protein disulfide isomerases to abrogate survival responses to endoplasmic reticulum stress. Cancer Research. 2008 Jul 1;68(13):5363–9.

26. Rosenbloom KR, Armstrong J, Barber GP, Casper J, Clawson H, Diekhans M, Dreszer TR, Fujita PA, Guruvadoo L, Haeussler M, Harte RA, Heitner S, Hickey G, Hinrichs AS, Hubley R, Karolchik D, Learned K, Lee BT, Li CH, Miga KH, Nguyen N, Paten B, Raney BJ, Smit AFA, Speir ML, Zweig AS, Haussler D, Kuhn RM, Kent WJ. The UCSC Genome Browser database: 2015 update. Nucleic Acids Res. 2015 Jan;43(Database issue):D670–81.

27. Oyadomari S, Mori M. Roles of CHOP/GADD153 in endoplasmic reticulum stress. Cell Death and Differentiation. 2004 Apr;11(4):381–9.

28. Nakagawa T, Zhu H, Morishima N, Li E, Xu J, Yankner BA, Yuan J. Caspase-12 mediates endoplasmic-reticulum-specific apoptosis and cytotoxicity by amyloid-beta. Nature. 2000 Jan 6;403(6765):98–103.

29. Salaün C, Leroy C, Rousseau A, Boitez V, Beck L, Friedlander G. Identification of a novel transport-independent function of PiT1/SLC20A1 in the regulation of TNF-induced apoptosis. J Biol Chem. 2010 Nov 5;285(45):34408–18.

30. Galligan JJ, Petersen DR. The human protein disulfide isomerase gene family. Hum. Genomics. 2012;6:6.

31. Schipani E, Ryan HE, Didrickson S, Kobayashi T, Knight M, Johnson RS. Hypoxia in cartilage: HIF-1alpha is essential for chondrocyte growth arrest and survival. Genes Dev. 2001 Nov 1;15(21):2865–76.

32. Masuda M, Miyazaki-Anzai S, Keenan AL, Shiozaki Y, Okamura K, Chick WS, Williams K, Zhao X, Rahman SM, Tintut Y, Adams CM, Miyazaki M. Activating transcription factor-4 promotes mineralization in vascular smooth muscle cells. JCI Insight. 2016 Nov 3;1(18).

33. Ellgaard L, Ruddock LW. The human protein disulphide isomerase family: substrate interactions and functional properties. EMBO Rep. 2005 Jan;6(1):28–32.

34. Hatahet F, Ruddock LW. Protein disulfide isomerase: a critical evaluation of its function in disulfide bond formation. Antioxid. Redox Signal. 2009 Nov;11(11):2807–50.

35. Hughes A, Oxford A, Tawara K, Jorcyk C, Oxford J. Endoplasmic Reticulum Stress and Unfolded Protein Response in Cartilage Pathophysiology; Contributing Factors to Apoptosis and Osteoarthritis. IJMS. 2017 Mar;18(3):665.

36. Wang W, Lian N, Li L, Moss HE, Wang W, Perrien DS, Elefteriou F, Yang X. Atf4 regulates chondrocyte proliferation and differentiation during endochondral ossification by activating Ihh transcription. Development. 2009 Dec;136(24):4143–53.

37. Cameron TL, Gresshoff IL, Bell KM, Piróg KA, Sampurno L, Hartley CL, Sanford EM, Wilson R, Ermann J, Boot-Handford RP, Glimcher LH, Briggs MD, Bateman JF. Cartilage-specific ablation of XBP1 signaling in mouse results in a chondrodysplasia characterized by reduced chondrocyte proliferation and delayed cartilage maturation and mineralization. Osteoarthr Cartil. 2015 Apr;23(4):661-70

38. Guo F-J, Xiong Z, Lu X, Ye M, Han X, Jiang R. ATF6 upregulates XBP1S and inhibits ER stress-mediated apoptosis in osteoarthritis cartilage. Cell Signal. 2014 Feb;26(2):332–42.

39. Pakos Zebrucka K, Koryga I, Mnich K, Ljujic M, Samali A, Gorman AM. The integrated stress response. EMBO Rep. 2016 Oct 4;17(10):1374–95.

40.   Freedman RB, Klappa P, Ruddock LW. Model peptide substrates and ligands in analysis of action of mammalian protein disulfide-isomerase. Meth. Enzymol. 2002;348:342–54.

41.   Kozlov G, Määttänen P, Thomas DY, Gehring K. A structural overview of the PDI family of proteins. FEBS Journal. 2010 Aug 26;277(19):3924–36.

42.   Vranka J, Mokashi A, Keene DR, Tufa S, Corson G, Sussman M, Horton WA, Maddox K, Sakai L, Bächinger HP. Selective intracellular retention of extracellular matrix proteins and chaperones associated with pseudoachondroplasia. Matrix Biol. 2001 Nov;20(7):439–50.

43.   Vertel BM, Velasco A, LaFrance S, Walters L, Kaczman-Daniel K. Precursors of chondroitin sulfate proteoglycan are segregated within a subcompartment of the chondrocyte endoplasmic reticulum. J Cell Biol. 1989 Oct;109(4 Pt 1):1827–36.

44.   Hecht JT, Hayes E, Snuggs M, Decker G, Montufar-Solis D, Doege K, Mwalle F, Poole R, Stevens J, Duke PJ. Calreticulin, PDI, Grp94 and BiP chaperone proteins are associated with retained COMP in pseudoachondroplasia chondrocytes. Matrix Biol. 2001 Jul;20(4):251–62.

45.   Bentovim L, Amarilio R, Zelzer E. HIF1 is a central regulator of collagen hydroxylation and secretion under hypoxia during bone development. Development. 2012 Dec 4;140(1):248–8.

46.   Han J, Back SH, Hur J, Lin Y-H, Gildersleeve R, Shan J, Yuan CL, Krokowski D, Wang S, Hatzoglou M, Kilberg MS, Sartor MA, Kaufman RJ. ER-stress-induced transcriptional regulation increases protein synthesis leading to cell death. Nat Cell Biol. 2013 May;15(5):481–90.

47.   Aro E, Khatri R, Gerard-O'Riley R, Mangiavini L, Myllyharju J, Schipani E. Hypoxia-inducible factor-1 (HIF-1) but not HIF-2 is essential for hypoxic induction of collagen prolyl

4-hydroxylases in primary newborn mouse epiphyseal growth plate chondrocytes. J Biol Chem. 2012 Oct 26;287(44):37134–44.

48. Maes C, Araldi E, Haigh K, Khatri R, Van Looveren R, Giaccia AJ, Haigh JJ, Carmeliet G, Schipani E. VEGF-independent cell-autonomous functions of HIF-1α regulating oxygen consumption in fetal cartilage are critical for chondrocyte survival. J Bone Miner Res. 2012 Feb 21;27(3):596–609.

49. Suzuki A, Ammann P, Nishiwaki-Yasuda K, Sekiguchi S, Asano S, Nagao S, Kaneko R, Hirabayashi M, Oiso Y, Itoh M, Caverzasio J. Effects of transgenic Pit-1 overexpression on calcium phosphate and bone metabolism. J Bone Miner Metab. 2010 Mar;28(2):139–48.

50. Byskov K, Jensen N, Kongsfelt IB, Wielsøe M, Pedersen LE, Haldrup C, Pedersen L. Regulation of cell proliferation and cell density by the inorganic phosphate transporter PiT1. Cell Div. 2012;7(1):7.

51. Kongsfelt IB, Byskov K, Pedersen LE, Pedersen L. High levels of the type III inorganic phosphate transporter PiT1 (SLC20A1) can confer faster cell adhesion. Exp Cell Res. 2014 May 28;:1–20.

52. Bourgine A, Colombeix C, Couasnay G, Masson M, Weiss P, Beck-Cormier S, Guicheux J, Beck L. Involvement of PiT1 and PiT2 in the phosphate sensing in osteoblastic cells. Bone. 2012 May;50:S70–0.

53. Chavkin NW, Chia JJ, Crouthamel MH, Giachelli CM. Phosphate uptake-independent signaling functions of the type III sodium-dependent phosphate transporter, PiT-1, in vascular smooth muscle cells. Exp Cell Res.; 2015 Feb 12;333:39–48.

54. Bon N, Couasnay G, Bourgine A, Sourice S, Beck-Cormier S, Guicheux J, Beck L. Phosphate (Pi)-regulated heterodimerization of the high-affinity sodium-dependent Pi

transporters PiT1/Slc20a1 and PiT2/Slc20a2 underlies extracellular Pi sensing independently of Pi uptake. J Biol Chem. 2018 Feb 9;293(6):2102-2114.

55.   Lau WL, Festing MH, Giachelli CM. Phosphate and vascular calcification: Emerging role of the sodium-dependent phosphate co-transporter PiT-1. Thromb. Haemost. 2010 Sep;104(3):464–70.

56.   Forand A, Beck L, Leroy C, Rousseau A, Boitez V, Cohen I, Courtois G, Hermine O, Friedlander G. EKLF-driven PIT1 expression is critical for mouse erythroid maturation in vivo and in vitro. Blood. 2013 Jan 24;121(4):666–78.

57.   Liu L, Sánchez-Bonilla M, Crouthamel M, Giachelli C, Keel S. Mice lacking the sodium-dependent phosphate import protein, PiT1 (SLC20A1), have a severe defect in terminal erythroid differentiation and early B cell development. Exp Hematol. 2013 May;41(5):432–7.

58.   Forand A, Koumakis E, Rousseau A, Sassier Y, Journe C, Merlin J-F, Leroy C, Boitez V, Codogno P, Friedlander G, Cohen I. Disruption of the Phosphate Transporter Pit1 in Hepatocytes Improves Glucose Metabolism and Insulin Signaling by Modulating the USP7/IRS1 Interaction. CellReports. 2016 Nov 8;17(7):1905.

59.   Bottger P, Pedersen L. The central half of Pit2 is not required for its function as a retroviral receptor. J Virol. 2004 Sep;78(17):9564–7.

60.   Bøttger P, Pedersen L. Evolutionary and experimental analyses of inorganic phosphate transporter PiT family reveals two related signature sequences harboring highly conserved aspartic acids critical for sodium-dependent phosphate transport function of human PiT2. FEBS J. 2005 Jun 1;272(12):3060–74.

29

61.   Bottger P, Pedersen L. Mapping of the minimal inorganic phosphate transporting unit of human PiT2 suggests a structure universal to PiT-related proteins from all kingdoms of life. BMC Biochem. 2011 ed. 2011;12:21.

62.   Farrell KB, Tusnady GE, Eiden MV. New structural arrangement of the extracellular regions of the phosphate transporter SLC20A1, the receptor for gibbon ape leukemia virus. J Biol Chem. 2009 Oct 23;284(43):29979–87.

Figure legends

Figure 1. *PiT1* deletion in growth plate cartilage impairs endochondral ossification. *(*A) Western-blot analysis of PiT1 and PiT2 expression in primary rib chondrocytes harvested 8h post-tamoxifen injection (8h p.i) at P3. *(B)* Safranin-O staining of humerus sections 7 days post-tamoxifen injection (7d p.i.) at P3; alcian blue staining and IHC for type II (Col II) and type X (Col X) collagen of humerus sections 19 days post-tamoxifen injection (19d p.i.). Main growth plate defects are indicated with white (proliferative zone) and black (hypertrophic zone) arrowheads. H, hypertrophic zone; P, proliferative zone. Scale bar, 200 μm. *(C)* RT-qPCR analysis of mRNA levels in primary rib chondrocytes harvested 24h p.i.. Data are expressed as means ± SEM **P< 0.01 versus Ctrl, n = 3. *(D)* mRNA levels of indicated genes in untransfected (Ctrl; black bars) or *PiT1*-depleted (shPiT1; white bars) ATDC5 cells differentiated during 28 days in presence of 10 μg/ml insulin, as assayed by RT-qPCR. Data are expressed as means ± SEM *P < 0.05, **P < 0.01 versus Ctrl, n = 4. (*E*) Alcian blue staining of Control (Ctrl) or *PiT1*-depleted (shPiT1) ATDC5 cells differentiated in presence of 10 μg/ml insulin. (*F*) Body weight of control and *PiT1^{cKO}* mice 19 d p.i. and gross appearance 19d p.i. *P < 0.05 versus Ctrl, n = 5.

Figure 2. *PiT1* depletion in cartilage induces ER-stress and chondrocyte death. *(*A) Alcian blue staining of humerus sections 8h p.i.. White arrowheads indicate intracellular alcian blue staining in the central region. Scale bar, 100μm. *(B)* Confocal images of ERp46 immunofluorescence (green) and aggrecan (red) on proximal humerus sections 8h p.i.. Central image shows the focal plane, lateral and bottom images are *xy* cross-sections. The intracellular retention of aggrecan in mutant chondrocytes is indicated with white arrowheads. Black arrowheads in controls indicate expected localization of aggrecan and ERp46. *(C)* Alcian blue staining of humerus sections 48h p.i.. Scale bar, 100μm. *(D)* Fluorescence detection of TUNEL-positive cells (*white arrowheads*) on humerus

sections 72h p.i.. Dashed lines indicate limits of hypertrophic zone (H). Scale bar, 100 μm. (*E*) Azur blue staining of transverse semi-thin sections of proximal humerus epiphysis from control and *PiT1^{cKO}* mice 8h p.i.. *(F)* Transmission electron micrographs of representative chondrocytes from the peripheral and central regions of the growth plate 8h p.i., as indicated. Black arrowheads indicate endoplasmic reticulum. Scale bar, 0.5 μm. *(G)* Immunohistochemistry for Chop (*left*) and caspase 12 (*right*) on growth plate central region of proximal humerus sections 8h p.i. Black arrowheads indicate positive signal. Scale bar, 50 μm. (*H*) RT-qPCR analysis of *PiT1, Chop, Atf4 and Bip* expression in primary chondrocytes isolated 8h p.i. Data are expressed as means ± SEM *P < 0.05, **P < 0.01 versus Ctrl, *n* = 3 per genotype. (*I*) *Xbp1* splicing in ATDC5 cells 24h after transduction with shScramble (*Ctrl*) or shPiT1 (*shPiT1*) lentivirus, as assayed by RT-PCR. Results show Xbp1s/Xbp1u ratios, normalized to the expression of the TATA box binding protein (Tbp) *P < 0.05 versus Ctrl, *n* = 4. (*J*) *RT*-qPCR analysis of *Chop* mRNA level in ATDC5 transfected with shScramble (*Ctrl*), shPiT1 (*shPiT1*) or Pi transport-deficient PiT1 mutant (*hPiT1-S621A*). Data were obtained 24h after transduction and are expressed as means ± SEM *P < 0.05 versus Ctrl, *n* = 3.

Figure 3. *PiT1* is an ER-stress regulated gene modulating Pdi activity. *(A)* Immunofluorescence detection of endogenous PiT1 (red) and ERp46 (green) in ATDC5 cells. Nuclei were stained with Hoechst (blue). (*B*) Western-blot analysis of PiT1 and Chop expression in ATDC5 treated (+Tm) or not (-Tm) with 2 μg/mL tunicamycin for 8h or 24h, *n*=3. *(C)* RT-qPCR analysis of *PiT1* mRNA levels in siRNA-transfected (100 nM) ATDC5 cells. Twenty-four hours after transfection, cells were treated (+Tm) or not (-Tm) with 2 μg/mL tunicamycin for 8h. Data are expressed as means ± SEM *P < 0.05 versus untreated siScramble-transfected (*siCtrl*) cells, *n* = 3. (*D*) Western-blot of PiT1 and Pdi after immunoprecipitation with anti-PDI or anti-PiT1 antibodies from tunicamycin-treated (+Tm) or untreated (-Tm) ATDC5 cells. (*E*) ATDC5 cells were transfected either with *shScramble* or *shPiT1* and Pdi activity was measured using an insulin reduction assay in ATDC5

protein lysates, supplemented or not with 1μg Pdi protein. The inset depicts the extinction coefficients. *(F)* Pdi activity as assayed using a cell-free insulin turbidity assay. Recombinant Pdi protein (1μg) and increasing PiT1 large intracellular loop (iLoop1) were incubated at increasing ratios. Turbidity was monitored at O.D. 660 nm. Dashed lines represent the reaction lag time threshold. The increase of turbidity after 45 min (means ± SEM *P < 0.05 versus Pdi alone, n = 3) is represented in the inset.

Figure 4. The ER-stress caused by *PiT1* deficiency is associated with decreased Vegf-A secretion in the central hypoxic region of the growth plate. (*A*) Immunofluorescence detection of Vegf-A (*red*) in proximal humerus sections of control and *PiT1^{cKO}* mice 8h p.i. Nuclei were stained with Hoechst (*blue*), n = 4. (B) RT-qPCR analysis of *Vegf-A* expression in epiphysis of control and *PiT1^{cKO}*mice 8h p.i., *n=3. (C)* RT-qPCR analysis of mRNA levels of indicated genes in primary chondrocytes from control and *PiT1^{cKO}* mice harvested 48h p.i. Cells were cultured under normoxic (21% O_2) or hypoxic (1% O_2) conditions during 8h before analysis. Data are expressed as means ± SEM *P < 0.05 versus 21% O2, n = 3. (*D*) ELISA detection of Vegf-A protein levels in the supernatant of primary chondrocytes from control and *PiT1^{cKO}* mice harvested 48h p.i. Cells were cultured under normoxic (21% O_2) or hypoxic (1% O_2) conditions during 24h before analysis. Data are expressed as means ± SEM *P < 0.05 versus 21% O_2, #P < 0.05 versus Ctrl, n = 3. (*E*) Quantification of Vegf-A protein expression in primary chondrocytes cultured under 1% O_2 during 24h, as assayed by western blotting (see Supplemental Fig. 4). Cells were transfected either with shScramble or shPiT1, together with empty plasmid (pcDNA6) of plasmid expressing wild-type (PiT1wt) or transport-deficient mutant (PiT1mut) PiT1, as indicated. Band intensity was normalized either using ß-actin or ß-tubulin. n = 3.

33

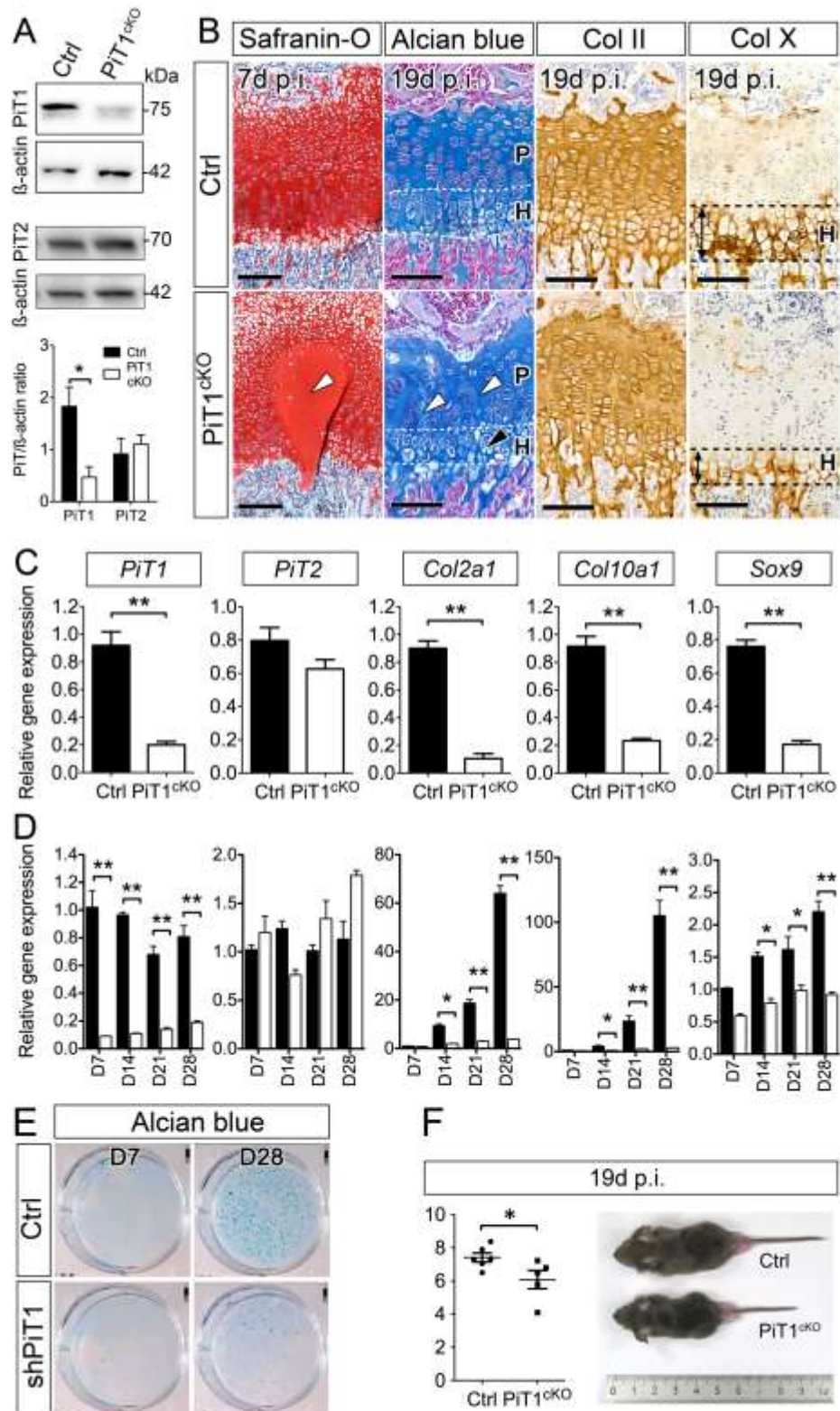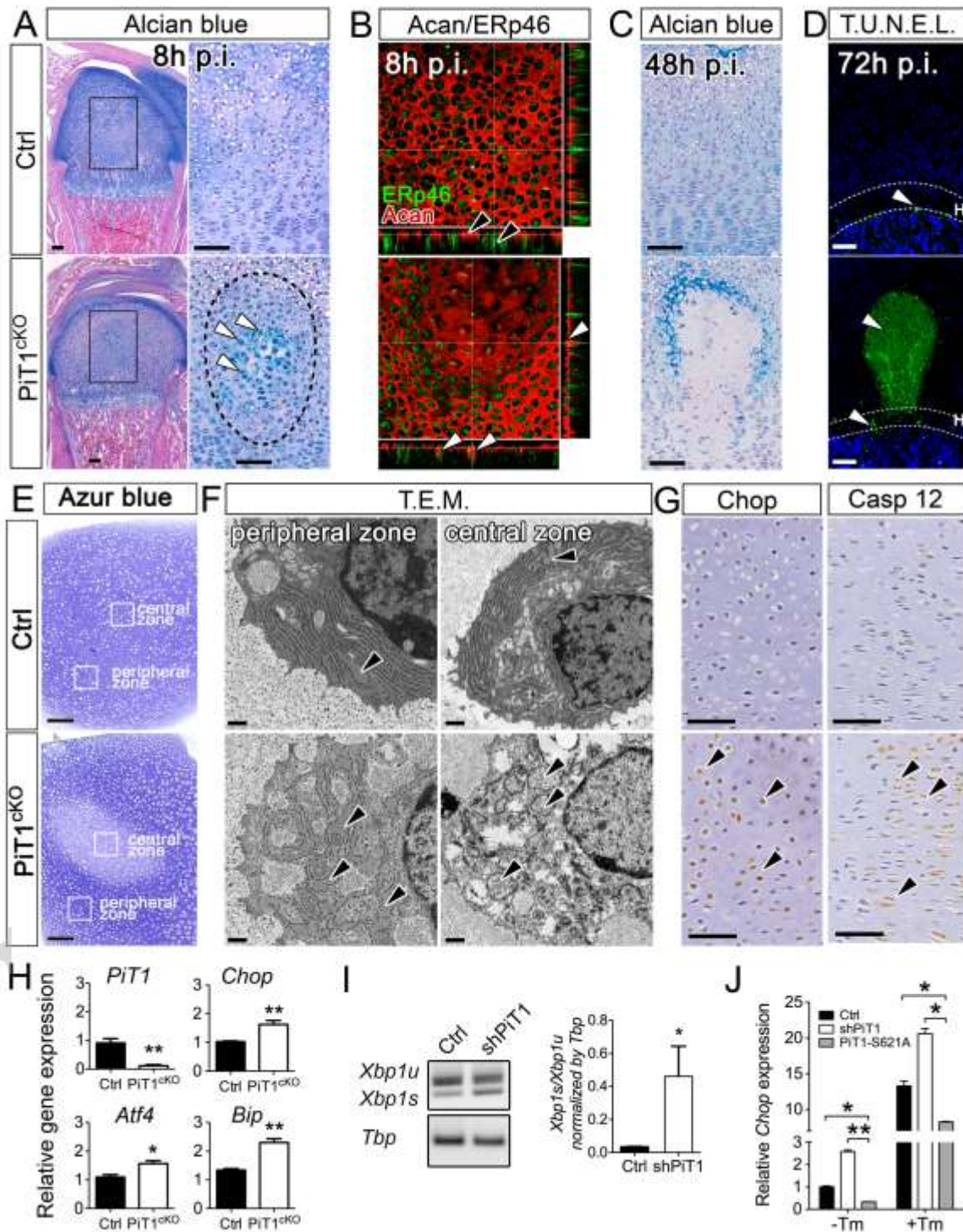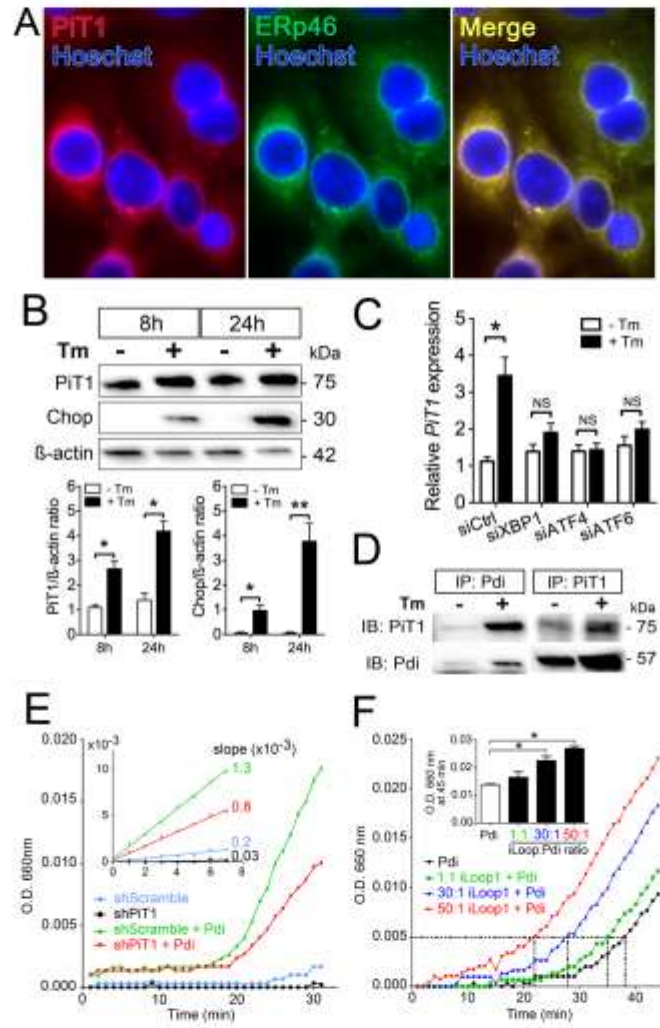Figure 1 - Couasnay *et al.*

Figure 2 - Couasnay *et al.*

Figure 3 - Couasnay *et al.*

Figure 4 - Couasnay *et al.*